American Journal of Analytical Chemistry, 2016, 7, 1-11
Published Online January 2016 in SciRes. http://www.scirp.org/journal/ajac
http://dx.doi.org/10.4236/ajac.2016.71001

Cathodic Using of ZrB_2-αSiC and TiB_2-αSiC for PEM Electrolysis and Water Electrolysis at Low Temperature

Kafoumba Bamba*, Nahossé Ziao

Laboratoire de Thermodynamique et de PHysico-Chimie du Milieu, UFR-SFA, Université Nangui Abrogoua, Abidjan, Côte d'Ivoire
Email: *bambakaf_sfa@una.edu.ci

Received 21 November 2015; accepted 12 January 2016; published 15 January 2016

Abstract

39 mol% SiC of ceramic pellets ZrB_2-αSiC and TiB_2-αSiC were synthesized by the reactive hot pressure RHP process at 1850˚C under 40 Mpa in vacuum. The XR diffraction displays the absence of other reagents apart from ZrB_2, SiC and TiB_2 confirming the purity of the pellets. The cathodic exploitation of both of them through electrochemical study shows that TiB_2-αSiC is the most active for Hydrogen Evolution Reaction (HER) and Hydrogen Oxidation Reaction (HOR) in 0.5 M of H_2SO_4 solution at room temperature. Moreover, the kinetic exploitation shows that for both pellets the system is controlled by mass transport when they are used as HER. However, in the case of HOR, the system is controlled by the electron transfer.

Keywords

Ceramic Pellets, HER, HOR, Polarization, Koutecky-Levich Plots

1. Introduction

Proton Exchange Membrane Fuel Cell PEMFC remains one of the competitive methods to produce a renewable energy up today. The combustible hydrogen provides a protected environmental clean energy; it is abundant and lightweight. The product from its oxidation that is water is environmentally benign [1]. The chemical energy per mass of hydrogen (142 MJ/Kg) is three times that of other chemical fuels like hydrocarbons (47 MJ/Kg). So far, its best production comes from the use of water as electrolyte according to the absence of monoxide carbon which is liable to depreciate the performance of the PEMFC [2] [3]. Therefore, the cleanest way for its produc-

*Corresponding author.

How to cite this paper: Bamba, K. and Ziao, N. (2016) Cathodic Using of ZrB_2-αSiC and TiB_2-αSiC for PEM Electrolysis and Water Electrolysis at Low Temperature. *American Journal of Analytical Chemistry*, **7**, 1-11.
http://dx.doi.org/10.4236/ajac.2016.71001

tion is to use sunlight in combination with photovoltaic cells and water electrolysis [4].

Considering these advantages, setting PEMFC requires however several attentions. We have the hydrogen storage, the efficiency of both electrodes, the tolerability of electrolyte toward electrodes and the efficiency of ion exchange membrane used. At the cathode of the cell, and because of their high activity for the hydrogen evolution reaction (HER), platinum/palladium black and carbon supported platinum or palladium nano-particles are most of the time used [5]-[7]. However, considering that the platinum remains the most expensive catalyst, doing without that precious material in the processes and replacing it by an active and cheap efficient electrode are a great desire to reduce the cost associated with the production of energy by electrochemical methods. Since then, many types of materials have also been used to reduce proton in hydrogen or to oxidize hydrogen. As the reaction is made in acidic area, those materials are confronted with corrosion [8]. Recently, Lonné *et al*. [9] experienced ceramic electrode based on ZrB_2-αSiC and coated with a proton conducting SiO_2-rich glass layer; they found a tremendous result with resistance and lack of corrosion in H_2SO_4 electrolyte but its polarization behavior toward reduction of hydrogen displays a high over-potential at about −0.5 V. Before, Monticelli *et al*. studied the corrosion asset of the naked ZrB_2-αSiC in aqueous solution. They found it a better candidate as a cathode electrode for hydrogen reduction and they emphasized on the anticorrosion asset of the ceramic that depends on the amount of SiC [10]. In this study, we test for the first time both ceramic components (61 mol% ZrB_2-αSiC and 61 mol% TiB_2-αSiC) as cathode rotating disk electrode RED for hydrogen evolution reaction HER and hydrogen oxidation reaction HOR in PEMFC.

Conductivity characteristic of ZrB_2-αSiC has been developed in previous articles emphasizing its resistance in corrosion even at high temperature (2000˚C), its high conductivity depending on the amount of α-SiC in the sample [11]-[14]. Whereas TiB_2-αSiC was described in other articles as exhibiting hardness, elastic modulus, high melting point and good corrosion resistance to chemical and oxidation resistance at temperature up to 1100˚C [15]-[17]. Therefore, the electrical conductivity of TiB_2-αSiC increases if the percentage of TiB_2 is more than that of α-SiC in the sample and decreases when temperature increases [18]. This value that is about 6.1 to 6.5×10^5 $S \cdot m^{-1}$ for a temperature between 25˚C and 927˚C is higher than that of ZrB_2-αSiC (2 $S \cdot m^{-1}$ at 80˚C).

2. Experimental

2.1. Sintering of ZrB_2-αSiC and TiB_2-αSiC

The starting reagents were TiB_2, ZrB_2 and α-SiC with respectively an average size of 1.2 - 2 µm, 4.7 - 5.3 µm and 0.7 - 1.0 µm. They were used as received with high purity about 98%+. Both ZrB_2-αSiC and TiB_2-αSiC were prepared according to the same protocol thanks to the route described explicitly in ref.9. Nevertheless, the sintering process has been slightly modified to well improve the density of the pellets. In fact, the sintering was made following a program.

First, during 1 h, the sample is heated with a slope of 15˚C/min from home temperature until 1000˚C. The High pressure 40 MPa equivalent of 1282 kg is then applied on the sample. The temperature dwelling at 1000˚C for 15 min, the heating is then pursued for 1 h always with the slope of 15˚C/min until 1850˚C. Then, this temperature is maintained during 2 hours whence the high pressure is stopped and the cooling starts with the slope of 30˚C/min. This final operation last out 1 h. **Figure 1** displays the detail program.

After cooling the samples, they are cleaned out of BN that was coated on the graphite die and weighted. Density of 98.7% for ZrB_2-αSiC and 99% for TiB_2-αSiC were obtained.

2.2. X-Ray Diffraction

After polishing the pellets, a D5000 diffractometer equipped with a Cu as the anticathode and a back monochromator was used for characterization. The wavelength used was λ = 1.5406 Å. The diffraction data were collected at a constant rate of 0.02˚ min^{-1} over an angle range of 2θ = 10˚ - 60˚.

2.3. Electrochemical Measurements

Cyclic voltammetric and polarization were carried out at room temperature in a standard three-electrode cell over a model 362 scanning potentiostat. The scanning was controlled by the software “potentiostat”. The solution was 0.5 M H_2SO_4 aqueous solution (Aldrich and Millipore MiliQ+ water). It was deoxygenated by bubbling pure nitrogen or argon to chase all trace of oxygen molecule. The reference electrode was RHE and the

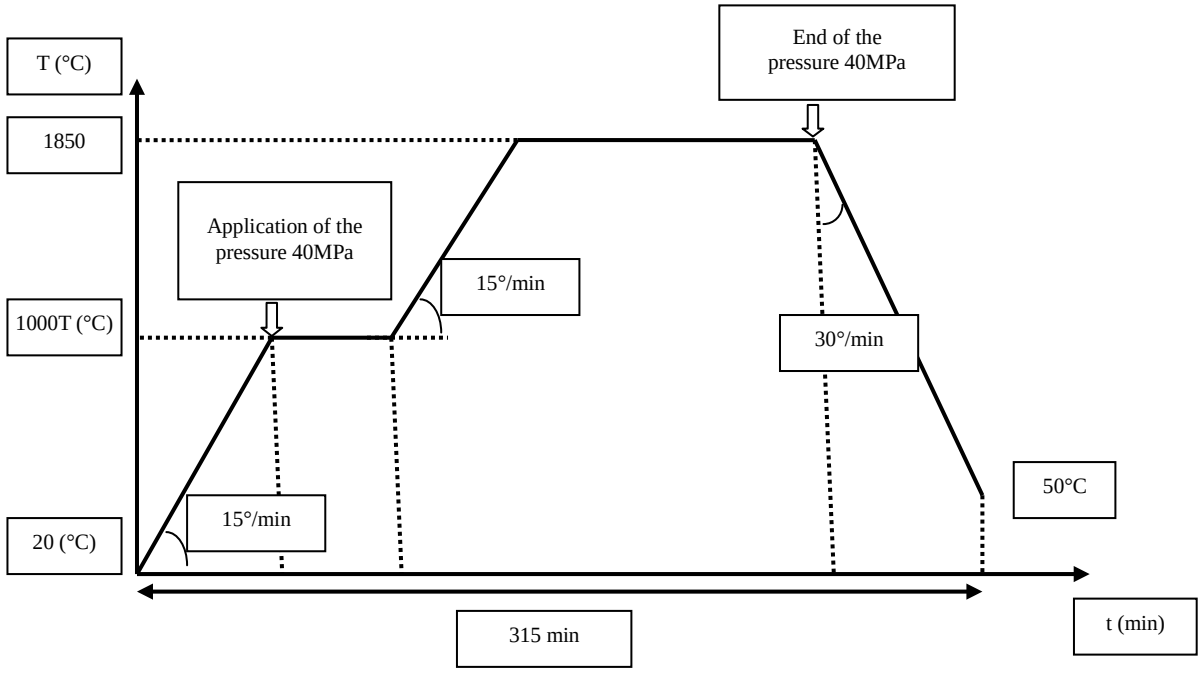

Figure 1. Sintering program of ZrB_2-αSiC and TiB_2-αSiC.

counter electrode was glassy carbon. The working electrode was the ceramic ZrB_2-αSiC and TiB_2-αSiC with geometry area of 18.46 mm^2, mounted on a rotating disc electrode RDE (CTV 101) provided by radiometer analytical. First the time, the pellets are surrounded by non conducting sheath (polyethylene, PTFE) constructed so that the faces of the electrode and the sheath are flush and only the face of disc electrode is in contact with the electrolyte solution. The speed of RDE for HER and HOR varies from 0 to 3000 rpm. The reactions on both ceramic catalysts were performed at quasi stationary conditions with sweep rate at 2 mV/s. The hydrogen was provided in the solution with a mass flow controller "Brooks 5850TR" (15 ml/min). Before recording the polarization, voltammery of bar platinum was carried out to notice the purity of the electrolyte with the sweep rate of 50 mV/s. The platinum used was a small disk with 0.15 cm^2 as geometric area.

3. Results and Discussion

3.1. Electrodes Constituents

After sintering and polishing the ceramic pellets, they were submitted to XRD diffraction. **Figure 2** displays their patterns.

Both pellets show that the α-SiC is present with a small amount. It is also shown that no compound apart from the reagents was detected. The patterns also confirm the resistance of reagents at the temperature higher than 1800˚C during high pressure HP sintering. This result has been confirmed by Zhao *et al*. [19].

3.2. Electrochemical Analyses

Ceramics pellets have been exploited to perform an electrochemical test. So, the RDE (2 $mv{\cdot}s^{-1}$, 0.5 M H_2SO_4, room temperature) measurements were performed to evaluate their electrocatalytic properties. The tests were undertaken at different rate between 0 to 3000 rounds per minute (rpm). They were also made both for hydrogen evolution reaction (HER) and for hydrogen oxidation reaction HOR.

3.2.1. Hydrogen Evolution Reaction

Many authors have been interested of the HER over different types of metal used as indicative electrode. So far, a consensus has not been reached on the predominant reaction mechanism for the electrochemical formation of hydrogen molecule resumed by the following reaction:

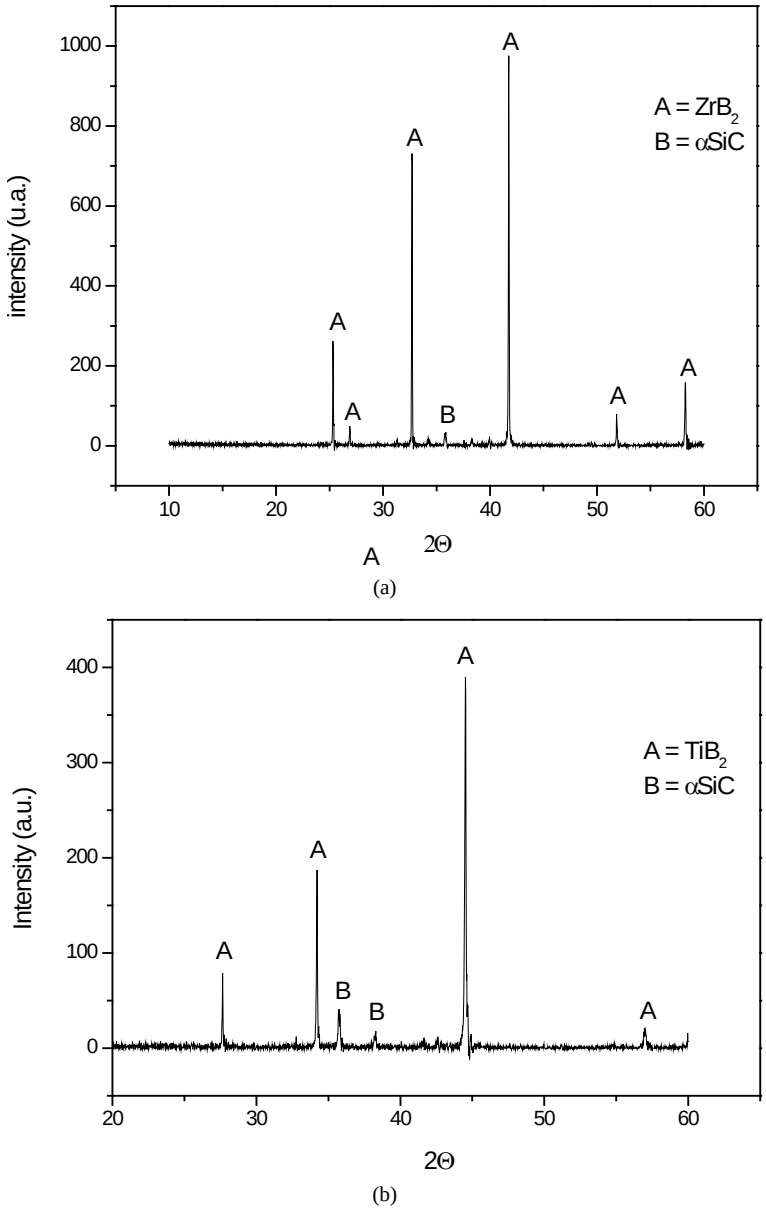

Figure 2. XRD of 61 mol% of (a) ZrB_2-αSiC; (b) TiB_2-αSiC.

$$2H^+ + 2e^- \rightarrow H_2 \quad [20]\text{-}[23] \tag{1}$$

This reaction is divided up through three electron transfer steps:

$$H^+ + e^- \rightarrow H_{ads} \quad \text{(Volmer)} \tag{2}$$

$$H_{ads} + H^+ + e^- \rightarrow H_2 \quad [24] \quad \text{(Heyrovsky)} \tag{3}$$

$$2H_{ads} \rightarrow H_2 \quad \text{(Tafel)} \tag{4}$$

The Volmer step (Equation (2)) that is the initial adsorption of the proton is admitted to be the fastest. And the subsequent step relies on two possible routes: the Tafel reaction (Equation (4)) is the homolytic step and the Heyrovsky (Equation (3)) that corresponds to the heterolytic step [23]. Nevertheless, the Tafel level is most of the time neglected assuming that the hydrogen is less adsorbed on the electrode surface for electrode made of Ni, Bi, C, etc. Therefore, the most common reactions held up are Volmer-Heyrovsky route [25] [26].

Figure 3 displays the polarization curves of ZrB_2-αSiC and TiB_2-αSiC as RDE at room temperature in acidic middle as explained above. The cathodic potential was comprised between 0 V to −1 V/RHE. Nevertheless, the potential was limited to −0.8 V/RHE for rotation speed less than 3000 rpm due to the existence of hydrogen at the electrode surface.

It shows that the hydrogen is produced at high overpotential when scanning in negative side. At 0 rpm regarding the steady-state, the potential is −0.541 V/RHE and −0.413 V/RHE over ZrB_2-αSiC (a) and TiB_2-αSiC (b) respectively. These values go down when the disk speed is high. They reach −0.417 V and −0.334 V/RHE at the rotation speed of 3000 rpm where the curves are well linear comparing to those at low speeds. This is caused by a lack of hydrogen bubbles formed by HER on the electrode surface that is responsible for the ohmic drop.

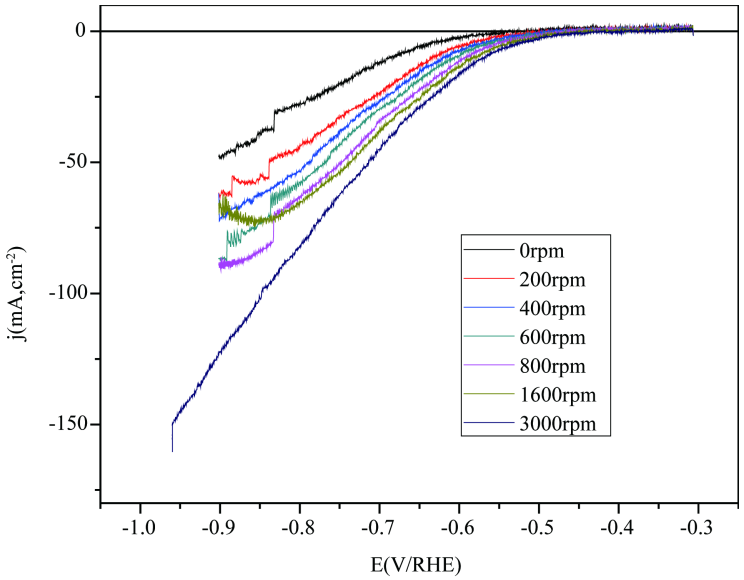

(a)

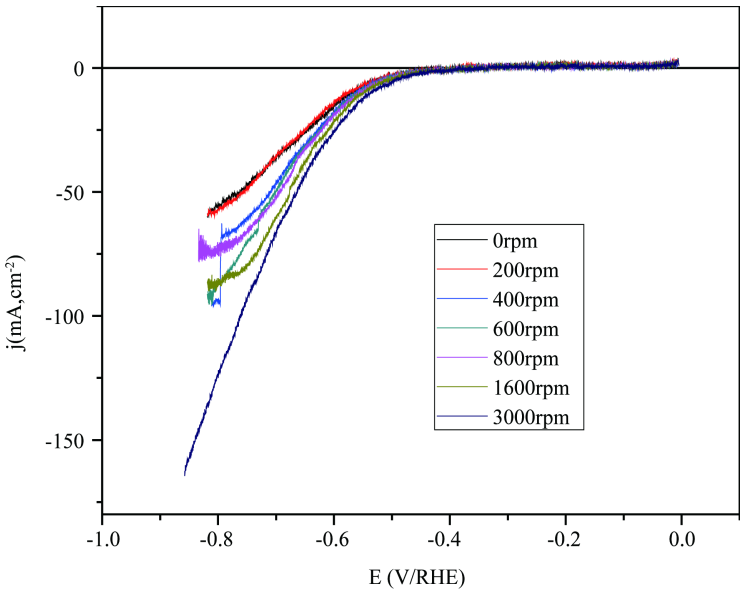

(b)

Figure 3. Polarization curves or linear voltammetry of (a) ZrB_2-αSiC and (b) TiB_2-αSiC mounted on RDE with various speeds at room temperature in H_2SO_4 0.5 M. These data were collected to construct the Koutechy-Lewich plot.

Moreover, the comparison of both pellets shows that TiB_2-αSiC is the most active since its activity requires low overpotential. Always at the speed of 0 rpm, comparison of both electrodes has been made with the linear voltammetry performed on bare platinum as displayed on **Figure 4**. It shows up that the bare platinum remains the most active electrode as sustained in literature [27]-[29]. Its overpotential for HER is −0.035 V and hydrogen production continues for −0.8 V without ohmic drop of the current. It means that the active sites of the platinum are not soon blocked up by hydrogen bubbles. Moreover, ZrB_2-αSiC displays not merely the highest overpotential but also its active sites are soon affected by hydrogen produced at its surface (−0.764 V) bringing out the ohmic drop.

The analysis of the curves was carried out using Koutecky-Levich equation:

$$\frac{1}{|j|}=\frac{1}{Bw^{1/2}}+\frac{1}{j_k} \tag{5}$$

where $B=0.62nFD_0^{2/3}\nu^{-1/6}C_0^*$ is the Levich constant and the slope of the equation, w is the RDE rate; j_k and j are respectively the kinetic (absence of mass transfer effect) and total current density at a given electrode potential. ν is the kinematic viscosity of the solution. Its value in aqueous middle is 10^{-2} $cm^2{\cdot}s^{-1}$ [30]; D_0 is the diffusion coefficient and C_0^* is the concentration of the solution. In fact, the current defined by Koutecky-Levich is the contribution of both diffusion and charge transfer currents.

$$\frac{1}{|j|}=\frac{1}{j_{dif}}+\frac{1}{j_k} \quad \text{with} \quad j_{dif}=Bw^{1/2}. \tag{6}$$

Figure 5 and **Figure 6** display the Koutecky plots of both ceramic electrodes. The linear plots obtained with the software Origin Pro 8 permit to determine for each potential the constant B and the current density j_k corresponding to the system when controlled by the electron transfer. From these plots, the total number of electron n can be calculated.

The **Table 1** displays the j_k, B and D_0 values coming of the Koutecky plots of both RDE electrodes for each potential.

Assuming that n is the total number of electron transferred during the hydrogen evolution, and the kinematic viscosity of the solution admitted to be 10^{-2} $cm^2{\cdot}s^{-1}$ for aqueous solution, we can calculate the diffusion coefficient for each value of B given in **Table 1** through the equation

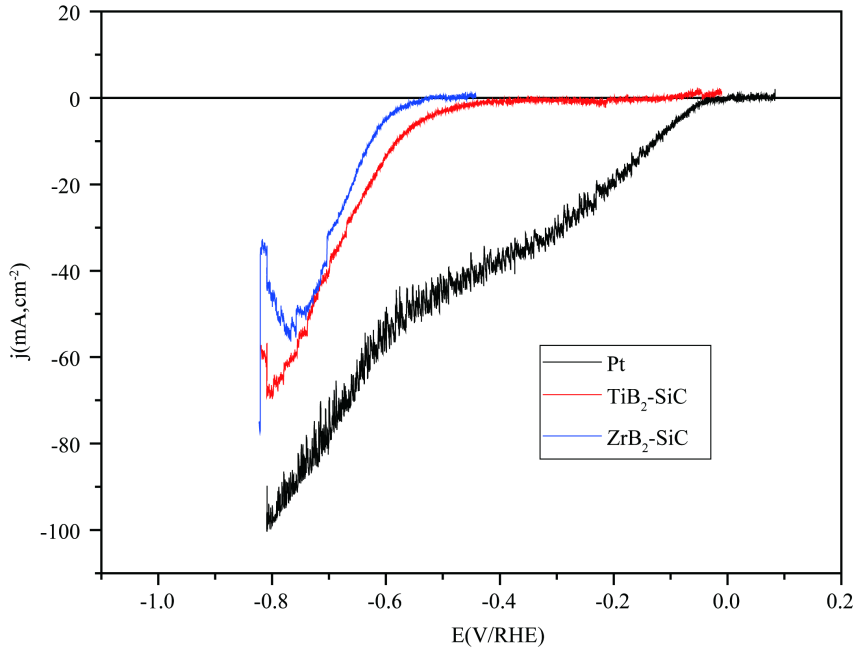

Figure 4. Linear voltammetry of Pt, TiB_2-αSiC and ZrB_2-αSiC in steady-state in H_2SO_4 0.5 M at room temperature (2 mV/s, 0 rpm).

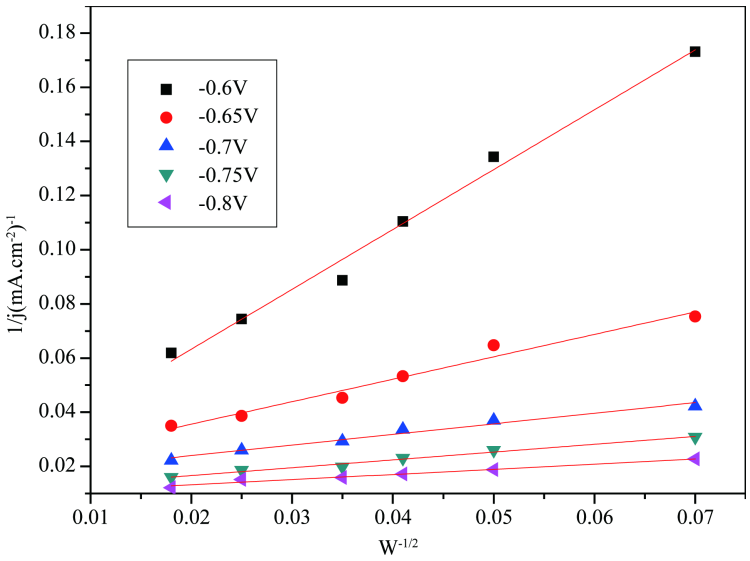

Figure 5. Koutecky-Levich plots 1/j vs. $w^{-1/2}$ for proton reduction at ZrB_2-αSiC rotating disk electrode (H_2SO_4 0.5 M, room temperature, 2 $mV \cdot s^{-1}$).

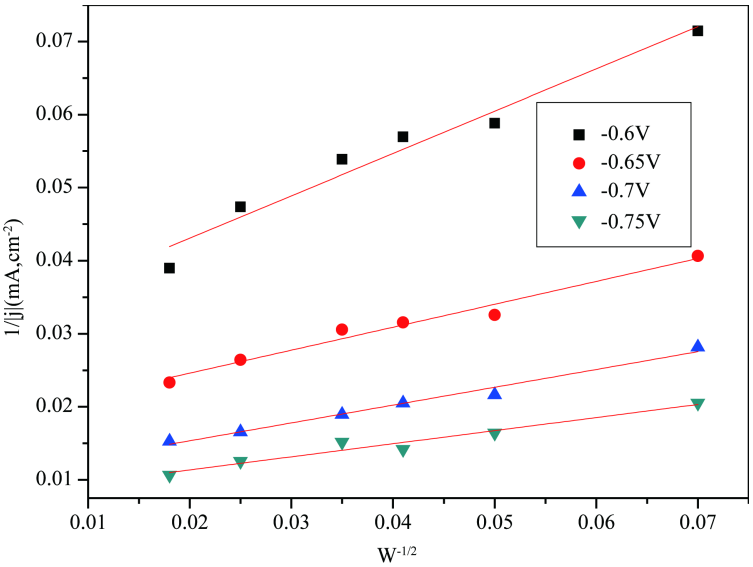

Figure 6. Koutecky-Levich plots 1/j vs. $w^{-1/2}$ for proton reduction at TiB_2-αSiC rotating disk electrode (H_2SO_4 0.5 M, room temperature, 2 $mV \cdot s^{-1}$).

Table 1. Kinetic parameters recorded with ZrB_2-αSiC and TiB_2-αSiC RDE for each overpotential.

Electrode	Parameters	Potential (V/RHE)				
		−0.60	−0.65	−0.70	−0.75	−0.80
ZrB_2-αSiC	$\|j_k\|$ ($mA \cdot cm^{-2}$)	52.30	52.50	69.40	92.00	106.20
	B	0.45	1.20	2.56	3.47	5.26
	D_0 (10^{-6} $cm^2 \cdot s^{-1}$)	0.85	3.70	12.00	18.00	34.00
TiB_2-αSiC	$\|j_k\|$ ($mA \cdot cm^{-2}$)	31.80	54.60	95.40	128.50	
	B	1.72	3.19	4.10	5.58	
	D_0 (10^{-6} $cm^2 \cdot s^{-1}$)	6.40	16.00	23.00	37.00	

$$D_0 = \left(\frac{B}{0.62nFAC_0^* \nu^{-1/6}} \right)^{3/2}. \quad (7)$$

The electrode geometric surface is 0.18 cm^2 for the pellets diameter of 4.85 mm.

3.2.2. Hydrogen Oxidation Reaction HOR

It is performed by bubbling and dissolving hydrogen gas through the electrolyte solution (0.5 M H_2SO_4). For each rate of the RDE, linear voltamogram was carried out from 0 to 3000 rpm. The limited potentials were −0.8 and 0 V/RHE with identical parameters during the HER. The potential sweep was 2 mV/s. The general equation concerning HOR in acidic solution is:

$$H_2 \leftrightarrows 2H^+ + 2e^-. \quad (8)$$

This reaction takes place at the interface through three recognized kinetic steps.

$$H_{2elec} \leftrightarrows 2H_{ads} \quad \text{is the Tafel step} \quad (9)$$

$$H_{2elec} \leftrightarrows H_{ads} + H_{aq}^+ + e^- \quad \text{is the Heyrovsky step} \quad (10)$$

$$\text{And the Volmer step is} \quad H_{ads} \leftrightarrows H_{aq}^+ + e^-. \quad (11)$$

Nevertheless, we can note the diffusion step of molecular hydrogen from bulk solution to the electrode surface $H_{2sol} \leftrightarrows H_{2elec}$. As there is no layer formed at ceramic electrodes surface during HOR, Tafel step will be neglected for weakly adsorption as well as in the HER reaction [16].

The **Figure 7** below displays the polarization curves of ZrB_2-αSiC. Before, a voltammetry of bare platinum was recorded in presence of argon atmosphere to confirm the purity of the bulk solution. The anodic potential was comprised between −0.9 V and 0 V/RHE. However, the potential was limited at 0 V because since −0.43 V/RHE, the limited current density was already reached with 8.4 $mA \cdot cm^{-2}$ regardless the rotation speed.

Figure 7 shows that apart from the steady sate, the curves are almost the same for each RDE speed. It shows that the HOR curves don't start with the same value of current as RDE speed increases and all the curves are

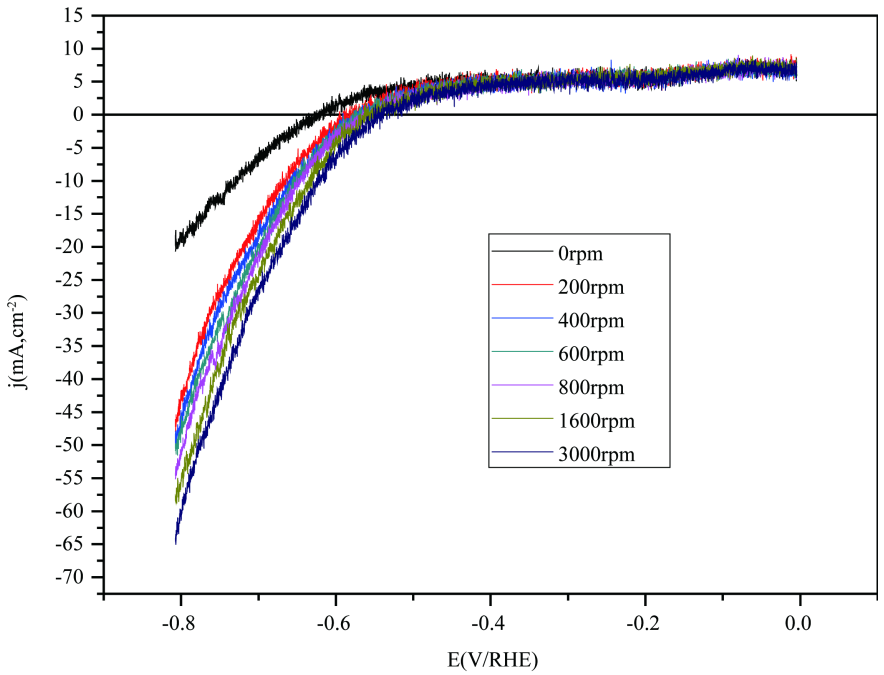

Figure 7. Hydrogen oxidation polarization at RDE ZrB_2-αSiC in 0.5 M H_2SO_4 at 2 mV/s and room temperature. H_2 saturated was dissolved in the electrolyte. The rotating speed varied between 0 rpm to 3000 rpm.

limited by the same current density (8.4 mA·cm^{-2}) from −0.508 V to 0.0 V/RHE although the rate of the rotating disk increases. This remark shows that the curves don't depend on the RDE rotation rate. Therefore, the system is not controlled by diffusion. Thus, the concentration of the dissolved hydrogen is the same in the bulk solution and at the electrode surface, regardless the electrode reaction.

Figure 8 displays the polarization curves of RDE TiB_2-αSiC. It has been recorded from −0.6 V to −0.2 V for electrode speeds comprised between 0 to 3000 rpm. It is observed as well as in **Figure 7** that there is no real difference between the curves when the speed increases. Therefore, we can conclude that the system doesn't depend on diffusion step.

The limit current recorded for each RDE rate is 4.91 mA·cm^{-2}. In this case, it is impossible to determine the Levich plots. Therefore, there is no proportionality between the limit current and the speed of the RDE. Then, to determine the kinetic parameters for ceramic electrodes during HOR, **Figure 9** displays the linear voltammograms of both electrodes at 0 rpm. It confirms that TiB_2-SiC is more active than ZrB_2-SiC with the limiting current reached respectively at −0.25 V/RHE and −0.0053 V/RHE.

4. Conclusions

In this study, non-oxide ceramic pellets ZrB_2-αSiC and TiB_2-αSiC with 39 mol% SiC were synthesized by hot pressure sintering methods at 1850˚C. The DRX performed on them shows the presence of only all raw materials used as ZrB_2, SiC and TiB_2 confirming their non-destruction and their purity. The electrocatalytic activity of both pellets was determined as rotating disk electrode for hydrogen evolution reaction (HER) and hydrogen oxidation reaction (HOR) for rotating speed comprised between 0 and 3000 rpm.

For HER characterization, we discover that the TiB_2-αSiC electrode is more active than ZrB_2-αSiC with production of hydrogen for an overpotential of −0.413 V/RHE and the current drop occurs by 0.8 V/RHE at a steady state in H_2SO_4 0.5 M solution. Moreover, the comparison with bare platinum with the same parameters reveals that the platinum remains the most active electrode with −0.035 V/RHE of overpotential.

Regarding HOR reaction, we found out that with both electrodes, the rotating disk is useless as the limit current observed remains the same regardless of the disk speed. It means that the determining step is not governed by diffusion.

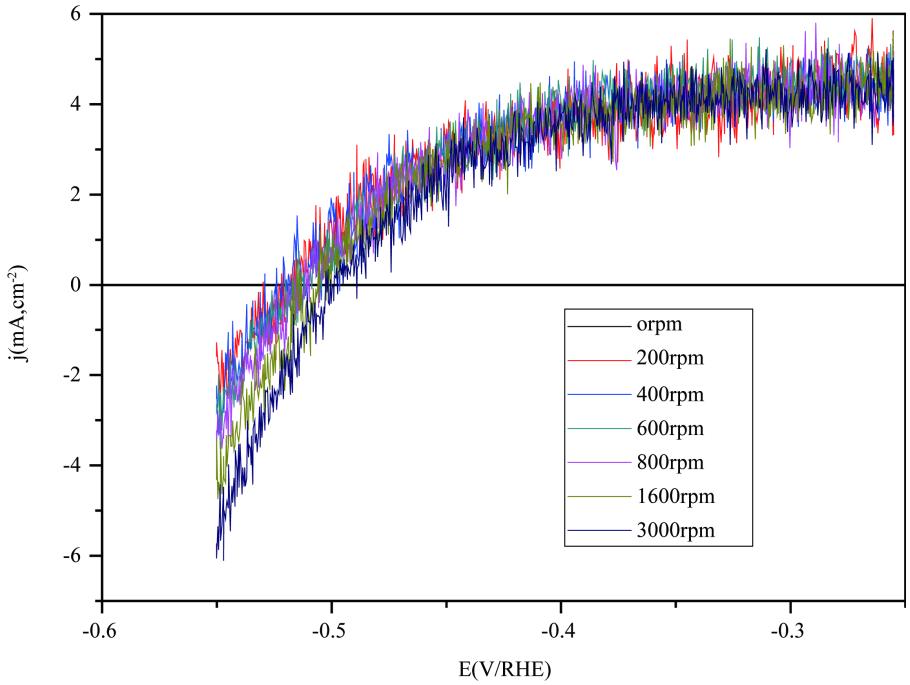

Figure 8. Hydrogen oxidation polarization at TiB_2-αSiC RDE in 0.5 M H_2SO_4 at 2 mV/s and room temperature. H_2 saturated was dissolved in the electrolyte. The rotating speed varied between 0 rpm to 3000 rpm.

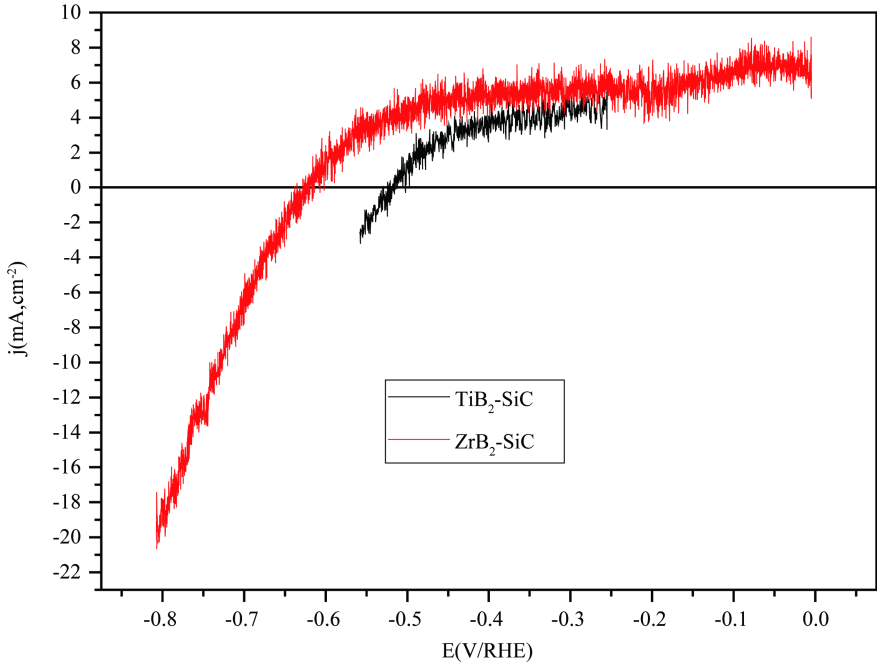

Figure 9. Linear voltammetry of TiB_2-αSiC and ZrB_2-αSiC in steady-state in H_2SO_4 0.5 M at room temperature (2 mV/s, 0 rpm) for HOR reaction.

On behalf of the resistance of both pellets in acidic middle, we need to vary the amount of αSiC in the compounds to increase the electrical conductivity. This will certainly reduce the overpotential for hydrogen evolution and make these ceramic electrodes better candidates as PEMFC electrodes than Pt electrode.

References

[1] Schlapbach, L. and Züttel, A. (2001) Hydrogen-Storage Materials for Mobile Applications. *Nature*, **414**, 353-358. http://dx.doi.org/10.1038/35104634

[2] Maillard, F., Peyrelade, E., Soldo-Olivier, Y., Chatenet, M., Chaînet, E. and Faure, R. (2007) Is Carbon-Supported Pt-WO_x Composite a CO-Tolerant Material? *Electrochimica Acta*, **52**, 1958-1967. http://dx.doi.org/10.1016/j.electacta.2006.08.024

[3] Micoud, F., Maillard, F., Gourgaud, A. and Chatenet, M. (2009) Unique CO-Tolerance of Pt-WO_x Materials. *Electrochemistry Communications*, **11**, 651-654. http://dx.doi.org/10.1016/j.elecom.2009.01.007

[4] Grätzel, M. (2001) Photoelectrochemical Cells. *Nature*, **414**, 338-344. http://dx.doi.org/10.1038/35104607

[5] Matsumoto, F. (2012) Ethanol and Methanol Oxidation Activity of PtPb, PtBi, and $PtBi_2$ Intermetallic Compounds in Alkaline Media. *Electrochemistry*, **80**, 132-138.

[6] Mayousse, E., Maillard, F., Foudo-Onana, F., Sicardy, O. and Guillet, N. (2011) Synthesis and Characterization of Electrocatalysts for the Oxygen Evolution in PEM Water Electrolysis. *International Journal of Hydrogen Energy*, **36**, 10474-10481. http://dx.doi.org/10.1016/j.ijhydene.2011.05.139

[7] Grigoriev, S.A., Millet, P. and Fateen, V.N. (2008) Evaluation of Carbon-Supported Pt and Pd Nanoparticles for the Hydrogen Evolution Reaction in PEM Water Electrolysers. *Journal of Power Sources*, **177**, 281-285. http://dx.doi.org/10.1016/j.jpowsour.2007.11.072

[8] Siroma, Z., Tanaka, M., Yasuda, K., Inaba, K. and Tasaka, A. (2006) Electrochemical Corrosion of Carbon Materials in an Aqueous Acid Solution. *Electrochemistry*, **75**, 258-260.

[9] Lonné, Q., Glandut, N., Labbe, J.-C. and Lefort, P. (2011) Fabrication and Characterization of ZrB_2-SiC ceramic Electrodes Coated with a Proton Conducting, SiO_2-Rich Glass Layer. *Electrochimica Acta*, **56**, 7212-7219. http://dx.doi.org/10.1016/j.electacta.2011.04.027

[10] Monticelli, C., Zucchi, F., Pagnoni, A. and Dal Colle, M. (2005) Corrosion of a Zirconium Diboride/Silicon Carbide Composite in Aqueous Solutions. *Electrochimica Acta*, **50**, 3461-3469. http://dx.doi.org/10.1016/j.electacta.2004.12.023

[11] Levine, S.R., Opila, E.J., Halbig, M.C., Kiser, J.D., Singh, M. and Salem, J.A. (2002) Evaluation of Ultra-High Temperature Ceramics Foraeropropulsion Use. *Journal of the European Ceramic Society*, **22**, 2757-2767. http://dx.doi.org/10.1016/S0955-2219(02)00140-1

[12] Yan, Y.J., Huang, Z.R., Dong, S.M. and Jiang, D.L. (2006) Pressureless Sintering of High-Density ZrB_2-SiC Ceramic Composites. *Journal of the American Ceramic Society*, **89**, 3589-3592. http://dx.doi.org/10.1111/j.1551-2916.2006.01270.x

[13] Rezaie, A., Fahrenholtz, W.G. and Hilmas, G.E. (2007) Effect of Hot Pressing Time and Temperature on the Microstructure and Mechanical Properties of ZrB_2-SiC. *Journal of Materials Science*, **42**, 2735-2744. http://dx.doi.org/10.1007/s10853-006-1274-2

[14] Han, J.C., Hu, P., Zhang, X.H., Meng, S.H. and Han, W.B. (2008) Oxidation-Resistant ZrB_2-SiC Composites at 2200 ˚C. *Composites Science and Technology*, **68**, 799-806. http://dx.doi.org/10.1016/j.compscitech.2007.08.017

[15] Tian, W., Kita, H., Hyuga, H., Kondo, N. and Nagaoka, T. (2010) Reaction Joining of SiC Ceramics Using TiB_2-Based Composites. *Journal of the European Ceramic Society*, **30**, 3203-3208. http://dx.doi.org/10.1016/j.jeurceramsoc.2010.07.017

[16] Blanc, C., Thevenot, F. and Goeuriot, D. (1999) Microstructural and Mechanical Characterization of SiC-Submicron TiB_2 Composites. *Journal of the European Ceramic Society*, **19**, 561-569. http://dx.doi.org/10.1016/S0955-2219(98)00227-1

[17] Zhao, G.L., Huang, G.Z., Liu, H.L., Zou, B., Zhu, H.T. and Wang, J. (2014) Microstructure and Mechanical Properties of TiB_2-SiC Ceramic Composites by Reactive Hot Pressing. *International Journal of Refractory Metals & Hard Materials*, **42**, 36-41. http://dx.doi.org/10.1016/j.ijrmhm.2013.10.007

[18] Li, W.J., Rong, T. and Goto, T. (2005) Preparation of TiB_2-SiC Eutectic Composite by an Arc-Melted Method and Its Characterization. *Materials Transactions*, **46**, 2504-2508. http://dx.doi.org/10.2320/matertrans.46.2504

[19] Zhao, G.L., Huang, C.Z., Liu, H.L., Zoua, B., Zhu, H.T. and Wang, J. (2014) A Study on *In-Situ* Synthesis of TiB_2-SiC Ceramic Composites by Reactive Hot Pressing. *Ceramics International*, **40**, 2305-2313. http://dx.doi.org/10.1016/j.ceramint.2013.07.152

[20] Markovic, N.M. and Ross Jr., P.N. (2002) Surface Science Studies of Model Fuel Cell Electrocatalysts. *Surface Science Reports*, **45**, 117-229. http://dx.doi.org/10.1016/S0167-5729(01)00022-X

[21] Kunimatsu, K., Senzaki, T., Tsushima, M. and Osawa, M. (2005) A Combined Surface-Enhanced Infrared and Electrochemical Kinetics Study of Hydrogen Adsorption and Evolution on a Pt Electrode. *Chemical Physics Letters*, **401**, 451-454. http://dx.doi.org/10.1016/j.cplett.2004.11.100

[22] Mukerjee, S., Srinivasan, S., Soriaga, M.P. and McBreen, J. (1995) Role of Structural and Electronic Properties of Pt and Pt Alloys on Electrocatalysis of Oxygen Reduction: An *in Situ* XANES and EXAFS Investigation. *Journal of the Electrochemical Society*, **142**, 1409-1422. http://dx.doi.org/10.1149/1.2048590

[23] Skulason, E., Karlberg, G.S., Rossmeisl, J., Bligaard, T., Greeley, J., Jonsson, H. and Norskov, J.K. (2007) Density Functional Theory Calculations for the Hydrogen Evolution Reaction in an Electrochemical Double Layer on the Pt(111) Electrode. *Physical Chemistry Chemical Physics*, **9**, 3241-3250. http://dx.doi.org/10.1039/b700099e

[24] Mello, R.M.Q. and Ticianelli, E.A. (1997) Kinetic Study of the Hydrogen Oxidation Reaction on Platinum and Nafion® Covered Platinum Electrodes. *Electrochimica Acta*, **42**, 1031-1039. http://dx.doi.org/10.1016/S0013-4686(96)00282-4

[25] Lasia, A. (2002) Applications of Electrochemical Impedance Spectroscopy to Hydrogen Adsorption, Evolution and Absorption into Metals. In: Conway, B.E. and White, R.E., Eds., *Modern Aspect of Electrochemistry*, Vol. 35, Chap. 1, Kluwer Academic Publishers, New York, 1-49. http://dx.doi.org/10.1007/0-306-47604-5_1

[26] Lasia, A. and Rami, A. (1990) Kinetics of Hydrogen Evolution on Nickel Electrodes. *Journal of Electroanalytical Chemistry and Interfacial Electrochemistry*, **294**, 123-141. http://dx.doi.org/10.1016/0022-0728(90)87140-F

[27] Croissant, M.J., Napporn, T., Léger, J.-M. and Lamy, C. (1998) Electrocatalytic Oxidation of Hydrogen at Platinum-Modified Polyaniline Electrodes. *Electrochimica Acta*, **16**, 2447-2457. http://dx.doi.org/10.1016/S0013-4686(97)10157-8

[28] Rau, M.S., Marozzi, C.A., Gennero de Chialvo, M.R. and Chialvo, A.C. (2010) Kinetic Study of the Hydrogen Oxidation Reaction on Membrane Coated Electrodes. Part II: Applications. *The Open Electrochemistry Journal*, **2**, 1-5. http://dx.doi.org/10.2174/1876505X01002010001

[29] Marozzi, C.A., Gennero-Chialvo, M.R. and Chialvo, A.C. (2009) Kinetic Study of the Hydrogen Oxidation Reaction on Membrane Coated Electrodes. Part I: Theoretical Aspects. *The Open Electrochemistry Journal*, **1**, 49-55. http://dx.doi.org/10.2174/1876505x00901010049

[30] Fatisson, J. (2005) Elaboration de nouveaux matériaux d'électrodes obtenus par autoassemblage de polyélectrolytes, nanoparticules et biomolécules: Etudes physico-chimiques et applications. Ph.D., University Joseph Fourier, Grenoble, 32.